

## Transition from Exponential to Nonexponential Kinetics during Formation of a Nonbiological Helix

Wei Yuan Yang, Ryan B. Prince, Jobiah Sabelko, Jeffrey S. Moore, and Martin Gruebele\*

School of Chemical Sciences and Beckman Institute for Advanced Science and Technology  
University of Illinois, Urbana, Illinois 61801

Received September 15, 1999  
Revised Manuscript Received February 24, 2000

Recently there has been considerable interest in synthetic peptides and other synthetic structure-forming oligomers as models for complex self-assembly and biopolymer folding.<sup>1–7</sup> We have measured the nanosecond folding kinetics of a phenylacetylene oligomer (PAO-12)<sup>8</sup> that is known to acquire a solvophobic driven helical structure<sup>4</sup> at low temperatures (Figure 1).

Folded PAO-12 is structurally organized by  $\pi$ - $\pi$  stacking interactions. We find that PAO-12 folds to a compact structure on a submicrosecond time scale, comparable to helical peptides.<sup>5</sup> In contrast to the peptides studied so far, it undergoes a transition to nonexponential kinetics at low temperatures. Since the thermodynamics and kinetics of this simple system are modeled only approximately by a two-state process  $H \rightleftharpoons U$ , we have developed a simple hexagonal lattice model that explains the salient features of our kinetics.

Solutions of PAO-12 were prepared at a concentration of 0.5  $\mu$ M in 50:50 (v/v) THF/methanol. This concentration and binary solvent avoids  $T$ -dependent aggregation, places the folding transition of the oligomer near room temperature, yet provides enough absorbance at 1.54  $\mu$ m for our  $T$ -jump studies. Steady-state fluorescence shows two peaks whose relative intensity varies with temperature, associated with the extended (350 nm) and folded (400 nm) conformations (Figure 1). The isobestic point is ill-defined, presumably due either to an intrinsic  $T$ -dependence of the fluorescence or to deviations from two-state equilibrium. Measurements of fluorescence baselines using nonfolding model compounds (e.g. PAO-2 or PAO-4) show that the former plays a role but cannot fully account for the deviations. Nonetheless, singular value decomposition<sup>9</sup> of the fluorescence profiles as a function of temperature reveals a cooperative sigmoidal transition between extended and self-assembled states, allowing the determination of an approximate experimental equilibrium constant  $K(T)$ .

Laser  $T$ -jump relaxation measurements probed the folding kinetics with the apparatus described by Ballew et al.<sup>10</sup> Incoming counterpropagating 1.54  $\mu$ m infrared pulses uniformly heated the

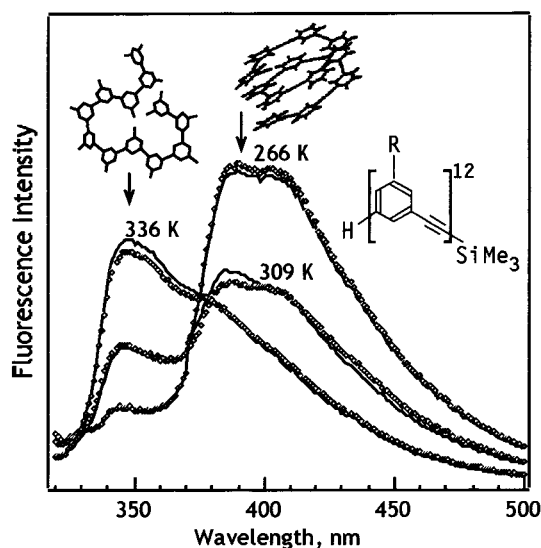


**Figure 1.** Emission spectra of PAO-12 (open diamonds) excited in the broad absorption band peaked at 270–300 nm are a diagnostic of its helical content.<sup>8</sup> ( $\lambda_{\text{exc}} = 288$  nm, 0.5  $\mu$ M PAO-12 in 50:50 (v/v) THF/methanol.) The folded peak at 400 nm decreases at higher  $T$ . A spectral/lattice model prediction (solid line) describes the folding transition and equilibrium constant near-quantitatively. Insets show representative unfolded and folded conformations, as well as the structural formula of PAO-12. R =  $-\text{CO}_2(\text{CH}_2\text{CH}_2\text{O})_3\text{CH}_3$ .

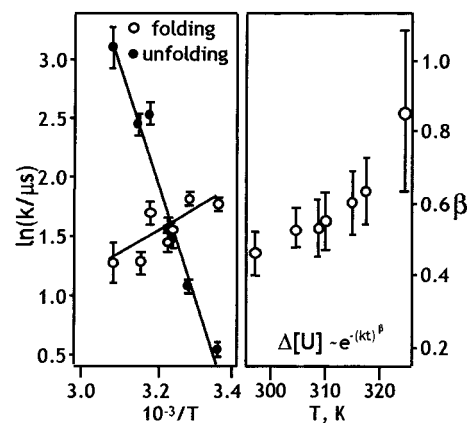


**Figure 2.** Left: Arrhenius plot of the approximate folding and unfolding rates of PAO-12. At low temperatures, the relaxation is better fitted by a stretched exponential or biexponential; the stretching exponent  $\beta$  is shown here as a convenient measure of the deviation from single exponentiality.

oligomer solution by 5 K in  $\approx 10$  ns (the dead-time). A mode-locked 280 nm laser pulse train induced oligomer fluorescence decays every 14 ns which were collected with 0.5 ns time resolution. A band-pass filter was used to monitor the increase in unfolded oligomer fluorescence in the 340–380 nm range.

Data in the 290–330 K range were fitted to single exponential, biexponential, and stretched exponential functions. The latter two gave significantly better agreement below 315 K. By combining the approximate exponential growth rates obtained from a single exponential fit ( $k_{\text{obs}} = k_f + k_b$ ) with the approximate equilibrium constant  $K = k_f/k_b$ , approximate forward and backward reaction rates were extracted as shown in the Arrhenius plot (Figure 2). Also shown is the value of  $\beta$  obtained by fitting the full transients to a stretched exponential:  $\beta$  is as a convenient measure of the extent to which the kinetics deviate from a single exponential at lower temperatures.

(1) Egholm, M.; Buchardt, O.; Nielsen, P. E.; Berg, R. H. *J. Am. Chem. Soc.* **1992**, *114*, 1895–1897.

(2) Cho, C. Y.; Moran, E. J.; Cherry, S. R.; Stephans, J. C.; Fodor, S. P.; Adams, C. L.; Sundaram, A.; Jacobs, J. W.; Schultz, P. G. *Science* **1993**, *261*, 1303–1305.

(3) Lokey, R. S.; Iverson, B. L. *Nature* **1995**, *375*, 303–305.

(4) Nelson, J. C.; Saven, J. G.; Moore, J. S.; Wolynes, P. G. *Science* **1997**, *277*, 1793–1796.

(5) Thompson, P. A.; Eaton, W. A.; Hofrichter, J. *Biochemistry* **1997**, *36*, 9200–9210.

(6) Kirshenbaum, K.; Barron, A. E.; Goldsmith, R. A.; Armand, P.; Bradley, E. K.; Truong, K. T.; Dill, K. A.; Cohen, F. E.; Zuckermann, R. N. *PNAS* **1998**, *95*, 4303–4308.

(7) Lednev, I. K.; Karnoup, A. S.; Sparrow, M. C.; Asher, S. A. *J. Am. Chem. Soc.* **1999**, *121*, 4076–4077.

(8) Prince, R. B.; Saven, J. G.; Wolynes, P. G.; Moore, J. S. *J. Am. Chem. Soc.* **1999**, *121*, 3114–3121.

(9) Henry, E. R.; Hofrichter, J. *Methods Enzymol.* **1992**, *210*, 129–192.

(10) Ballew, R. M.; Sabelko, J.; Reiner, C.; Gruebele, M. *Rev. Sci. Instrum.* **1996**, *67*, 3694–3699.

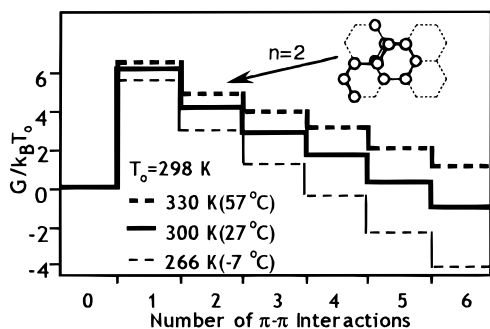


**Figure 3.** Free energy profiles derived from the lattice model described in the text and the Supporting Information. The folded side of the barrier slopes to the folded state very gently. Numerous small barriers ( $\approx k_B T$ , not shown) connect planar states with different  $n$ . A representative planar lattice conformer is shown.

The approximate folding rate  $k_f$  decreases slightly with increasing temperature, indicating that the folding free energy barrier is slowly increasing with  $T$ . This is consistent with the picture that the transition state must contain a structurally constrained turn with at least one  $\pi$ - $\pi$  stacking interaction, such that a higher entropic free energy cost is incurred as  $T$  is increased. The unfolding rate speeds up dramatically at higher temperatures as the compact state is destabilized.

The lack of a well-defined isosbestic point and single-exponential kinetics, and extrapolation of the Arrhenius plots to unrealistically large prefactors, are not consistent with simple two-state behavior. To better explain the folding process, a three-parameter hexagonal lattice model was constructed.<sup>11</sup> The model *explicitly* enumerates only planar and  $\pm 90^\circ$  twisted states (inset in Figure 3 shows a planar state on its lattice). Each planar segment lies on its own hexagonal lattice, and long-range steric hindrance is neglected. We adopted the energy function

$$E_i(n,m) = n\epsilon + mJ \quad (1)$$

where  $n$  counts the stacking interactions of energy  $\epsilon$ , and  $m$  counts the  $90^\circ$  twists of energy  $J$ . All conformers “ $i$ ” of this model can be enumerated explicitly. Forcing PAO-12 onto a lattice underestimates the entropy of “free” residues compared to “helix” residues, and we correct this with a degeneracy factor  $\alpha_i^{f_i}$ , where  $f_i$  counts the number of monomers in conformer “ $i$ ” not part of a helix.<sup>11</sup> With the model partition function

$$Z = \sum_i \alpha_i^{f_i} \exp(-E_i(n,m)/k_B T) \quad (2)$$

in hand, all thermodynamic quantities can be evaluated as a function of  $\epsilon$ ,  $J$ , and  $\alpha$ . Using a spectral model based on experimental data to describe the dependence of the spectrum on  $n$ ,<sup>11</sup> values of  $\epsilon = (-3.7 \pm 1)k_B T_0$  and  $\alpha = 2.7 \pm 1$  were obtained by directly fitting to the spectra as a function of  $T$  (Figure 1).  $J$  was fixed at  $0.861k_B T_0$  ( $T_0 = 298$  K) based on gas-phase measurements.<sup>12</sup> The fitted value of  $\epsilon$  is close to the gas-phase value for benzene stacking interactions ( $-2.7k_B T_0$ ),<sup>13</sup> indicating a relatively small solvent shift. The model equilibrium constant yields spectra in close agreement with experiment (Figure 1).

By grouping states according to  $n$  as the reaction coordinate, a one-dimensional free energy plot is obtained in Figure 3. The lattice model indicates that the free energy barrier is reached with a single stacking interaction. On the “folded” side of the barrier, the free energy slopes down slowly as  $n$  approaches 6. Partially folded states can interconvert over  $\approx k_B T$  barriers while folding and unfolding over the transition state barrier occurs: A Monte Carlo (MC) simulation using the lattice model<sup>11</sup> shows a non-exponential change in the  $n = 6$  concentration. Examination of the MC trajectories indicates that the kinetic behavior at low temperatures is due to a separation of the time scales for equilibration of partially folded states and for unfolding, which can be approximated by a sequential process  $H \rightleftharpoons P \rightleftharpoons U$ .

PAO-12 differs from helical peptides in that isomerization has a significant enthalpic barrier  $J$ , and 6 rather than 3–4 residues are involved in a turn. One would expect these factors to slow folding, yet the approximate time scale and overall activation barrier of a few  $k_B T$  do resemble the behavior of  $\alpha$ -helix folders.<sup>5,13,14</sup> Apparently these effects are offset by the higher rigidity of the PAO-12 structure. The ability to control barriers, interaction energies, and chirality by the use of substituents makes PAOs ideal model compounds for future studies of how structure and energetics affect folding into simple secondary structures.

**Acknowledgment.** This work was supported by the Dreyfus foundation, NIH R01 GM57175 (W.Y.Y., J.S., and M.G.) and NSF CHE 97-27172 (R.B.P. and J.S.M.).

**Supporting Information Available:** Details of the thermodynamic, spectral, and Monte Carlo kinetic modeling (PDF). This material is available free of charge via the Internet at <http://pubs.acs.org>.

JA993343+

(11) The model and fitting procedures are described in more detail in the Supporting Information; we were not able to describe the kinetics measured here with standard standard helix-coil models [e.g.: Poland D.; Scheraga H. A. *Theory of Helix-Coil Transitions in Biopolymers*; Academic Press: New York, 1970].

(12) Katsuhiko, O.; Hasegawa, T.; Ito, M.; Mikami, N. *J. Phys. Chem.* **1984**, *88*, 1711–1716.

(13) Neusser, H. J.; Krause, H. *Chem. Rev.* **1994**, *94*, 1829–1843.

(14) Williams, S.; Causgrove, T. P.; Gilmanshin, R.; Fang, K. S.; Callender, R. H.; Woodruff, W. H.; Dyer, R. B. *Biochemistry* **1996**, *35*, 691–697.